Elastic and inelastic conductance in Co-Fe-B/MgO/Co-Fe-B magnetic tunnel junctions

Ayaz Arif Khan, J. Schmalhorst,* and G. Reiss
Thin Films and Physics of Nanostructures, Department of Physics, Bielefeld University, P.O. Box 100131, 33501 Bielefeld, Germany

G. Eilers and M. Münzenberg
I. Physikalisches Institut, Georg-August-Universität Göttingen, Friedrich-Hund-Platz 1, 37077 Göttingen, Germany

H. Schuhmann and M. Seibt
IV. Physikalisches Institut, Georg-August-Universität Göttingen, Friedrich-Hund-Platz 1, 37077 Göttingen, Germany
(Received 8 April 2010; revised manuscript received 8 June 2010; published 13 August 2010)

A systematic analysis of the bias voltage and temperature dependence of the tunneling magnetoresistance (TMR) in Co-Fe-B/MgO/Co-Fe-B magnetic tunnel junctions with barrier thickness t_B between 1.8 and 4.0 nm has been performed. The resistance measured at low temperature in the parallel state shows the expected exponential increase with increasing barrier thickness. The low-temperature TMR amplitude of about 300% is quite similar for all MgO thicknesses. This is in accordance with microstructural investigations by transmission electron microscopy, which do not give hints to a reduction in the barrier quality with increasing MgO thickness. Both the junction resistance and TMR decrease with increasing temperature and bias voltage. In general, the decrease is much stronger for thicker barriers, e.g., a decrease in the TMR by a factor of 13.4 from 293% at 15 K to 21.9% at 300 K was observed for t_B=4.0 nm compared to a reduction by only a factor of 1.6 for t_B=1.8 nm. This behavior can be described self-consistently for all barrier thicknesses within a model that extends the magnon-assisted tunneling model by adding an inelastic, unpolarized tunneling contribution. Furthermore we discuss our results in the framework of a recent model by Lu *et al.* [Phys. Rev. Lett. **102**, 176801 (2009)] claiming that polarized hopping conductance becomes important for larger MgO thickness.

DOI: 10.1103/PhysRevB.82.064416 PACS number(s): 85.30.Mn

I. INTRODUCTION

The tunnel magnetoresistance (TMR) effect in magnetic tunnel junctions (MTJs) has been the subject of intensive research in both fundamental and applied physics. Investigating the TMR effect is very important for developing magnetic random access memory, magnetic sensors, and novel programmable logic devices.[1] This stimulated tremendous activity in the experimental and theoretical investigation of electronic, magnetic, and transport properties of MTJs. The TMR effect in MTJs has been known from the experiment of Julliere for almost 35 years.[2] Basing on the pioneering work by Parkin *et al.*,[3] Yuasa *et al.*,[4] and Djayaprawira *et al.*[5] nowadays well-oriented (001) MgO-based MTJs show a TMR ratio of more than 1000% at low temperature and 600% at room temperature (RT),[6,7] which accords with theoretical predictions basing on coherent tunneling.[8,9] In this type of junction the as-deposited Co-Fe-B electrodes are amorphous. They recrystallize[10,11] during a postannealing process using the MgO as a template for forming a (001) out-of-plane-oriented quasiepitaxial structure, which is crucial for coherent tunneling processes. It is well know that the diffusion of boron out of Co-Fe-B is necessary for proper crystallization of the electrode.[12,13] It has been reported in literature that B diffusion in MgO during postannealing process forms an intermediate MgB_xO_y oxide, where the B has an oxidation state close to B^{3+}.[13–15] Localized electronic states in the barrier may arise from these ionized boron species or even from oxygen vacancies.[16]

In addition to direct spin-polarized tunneling through the oxide, localized state (LS) in the barrier can lead to new current channels such as resonant tunneling or inelastic hopping via chains of localized states.[17–19] Depending on the barrier thickness, on the distribution of the electronic states localized in space and energy and on the temperature and bias voltage the relative contribution of these additional channels to the total conductance of an MTJ may range from negligible to dominant. With respect to the TMR amplitude it is of special importance, whether new current channels are spin conserving or not.

In this paper, we present a systematic study of the area resistance (RA) product and the TMR in Co-Fe-B/MgO/Co-Fe-B MTJs showing a maximal TMR of about 300% as a function of temperature and bias voltage. We show that in addition to direct spin-polarized and magnon-assisted tunneling dominating the transport for a barrier thickness of 1.8 nm the relative contribution of inelastic, unpolarized hopping becomes much more important with increasing barrier thickness. Our results will also be compared to results recently published by Lu *et al.*[14] on Co-Fe-B/MgO/Co-Fe-B MTJs showing a maximal TMR of 136%.

II. EXPERIMENT

The MTJ stacks were prepared in a magnetron sputtering system with a base pressure of 1×10^{-7} mbar. The layer stack is Ta(5)/Ru(30)/Ta(10)/Ru(10)/Mn-Ir(12)/Co-Fe-B(2.5)/MgO(t_B)/Co-Fe-B(2.5)/Ta(5)/Ru(20) on top of thermally oxidized (50 nm) silicon (100) wafers, where the target compositions of Mn-Ir and Co-Fe-B were $Mn_{83}Ir_{17}$ and $Co_{40}Fe_{40}B_{20}$, respectively. The numbers in parenthesis represent the nominal thickness of each layer in nanometer. All metallic layers were deposited by dc magnetron sputtering at

TABLE I. Typical RA_P and RA_{AP} products in the parallel and antiparallel magnetization state and the corresponding TMR measured with a bias voltage of 5 mV at 15 K and 300 K, respectively.

t_B (nm)	RA_P @ 15 K	RA_{AP} @ 15 K	TMR @ 15 K (%)	RA_P @ 300 K	RA_{AP} @ 300K	TMR @ 300K (%)
1.8	110 kΩ μm^2	421 kΩ μm^2	283	105 kΩ μm^2	291 kΩ μm^2	177
2.1	346 kΩ μm^2	1.34 MΩ μm^2	287	312 kΩ μm^2	843 kΩ μm^2	170
3.0	77.2 MΩ μm^2	311 MΩ μm^2	303	44.5 MΩ μm^2	76.7 MΩ μm^2	72.4
4.0	27.5 GΩ μm^2	108 GΩ μm^2	293	7.13 GΩ μm^2	8.69 GΩ μm^2	21.9

an Ar pressure of 1.2×10^{-3} mbar. The MgO barrier was deposited by rf magnetron sputtering at an Ar pressure of 2.4×10^{-2} mbar. Five wafers with different MgO thickness (t_B) were prepared (t_B=1.8, 2.1, 3.0, 4.0, and 5.0 nm). In order to activate the exchange bias of the hard electrode and the partial recrystallization of the electrodes the MTJs were annealed at 350 °C in the presence of a magnetic field (6.5 kOe) in a vacuum furnace with a base pressure of 1×10^{-7} mbar. The junctions with a size of 15×15 and 20×20 μm^2 were patterned by laser lithography and ion-beam etching. The transport properties of the MTJs were measured using the conventional two-probe technique with constant dc bias voltage in a closed cycle helium cryostat (Oxford Cryo drive 1.5) with a temperature range of 13–330 K. We also measured the dielectric stability of the MTJs at room temperature by performing time-dependent voltage ramp experiments.[20,21] At the breakdown voltage U_{BD}, the resistance of the MTJ shows an abrupt decrease because a highly conducting path is irreversibly produced.

The average values and statistical errors of the TMR amplitudes and area resistance products in the parallel state measured at room temperature are 173 ± 5 % and 106 ± 10 kΩ μm^2 for t_B=1.8 nm, 167 ± 4 % and 323 ± 18 kΩ μm^2 for t_B=2.1 nm, 73.2 ± 4.0 % and 43.4 ± 3.2 MΩ μm^2 for t_B=3.0 nm, and 22.5 ± 2.3 % and 6.09 ± 1.04 GΩ μm^2 for t_B=4.0 nm. The resistance of the sample with 5.0 nm barrier thickness was just too high (it was estimated to be about 30 TΩ μm^2 at low temperature) to perform reliable TMR measurements.

Structural analysis was carried out by using high-resolution transmission electron microscopy (HRTEM). The HRTEM cross-sectional samples were prepared by conventional focused ion-beam technique with a FEI NOVA NANOLAB 600, which allows sample preparation out of any desired region of our MTJs. The TEM work was done using a Philips CM200-FEG-UT operated at an acceleration voltage of 200 kV.[22]

III. RESULTS AND DISCUSSION

A. Transport properties

The resistance area product in the parallel (antiparallel) magnetic state RA_P(RA_{AP}) and the TMR of typical MTJs acquired at 15 and 300 K with a bias voltage of 5 mV are listed in Table I. These MTJs will be analyzed in detail with respect to their temperature and bias voltage dependence below. Exemplary TMR loops for t_B=1.8 and 4.0 nm measured at 15 and 300 K are shown in Fig. 1. The low-temperature TMR is very similar for all barrier thicknesses but the TMR temperature dependence becomes stronger with increasing t_B as can be seen in Fig. 2(b): whereas for t_B=1.8 nm the TMR drops from 283% at 15 K to 177% at 300 K, a decrease from 293% down to 21.9% is observed for t_B=4.0 nm. For t_B=3.0 nm an intermediate behavior (303% at 15 K to 72.4% at 300 K) was found. With respect to the TMR temperature dependence it is worth to note that the reduction in RA products for elevated temperature is always larger for antiparallel than for parallel magnetic state: whereas R^P is reduced by a factor of 1.05 only for t_B=1.8 nm between 15 and 300 K, it goes down by a factor of about 12.4 for t_B=4.0 nm in the antiparallel state. The low-temperature bias voltage dependence of TMR [see Fig. 2(a)] shows the same trend as the TMR temperature dependence, it becomes much stronger with increasing barrier thickness. Particularly, for t_B=4.0 nm the TMR nearly vanishes for bias voltage $|V|\geq500$ mV.

Another hallmark for the junction quality is its dielectric stability under voltage stress. The breakdown voltage listed in Table II increases nearly linearly with barrier thickness as it is expected by the E model.[23] Therefore, the intrinsic dielectric properties of the oxide are conserved at least up to t_B=5 nm. Finally, as expected the low-temperature RA product depends exponentially on barrier thickness: by fitting the logarithm of RA_P with a linear function ($\ln[RA_P(t_B)]=\gamma+\alpha t_B$, RA_P given in Ω μm^2) an exponential prefactor of $\alpha=6.1\pm0.2$ nm^{-1} ($\gamma=0.2\pm0.6$) was found which matches quite well with the data of Yuasa *et al.*[4] (α=6.41 nm^{-1}) who deposited their MgO barriers by electron-beam evaporation instead of rf sputtering.

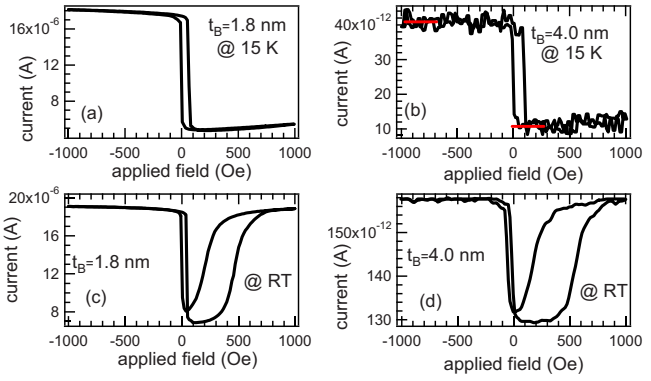

FIG. 1. (Color online) Typical dependence of the current on the applied magnetic field acquired with 5 mV bias voltage measured at 15 and 300 K for t_B=1.8 and 4.0 nm.

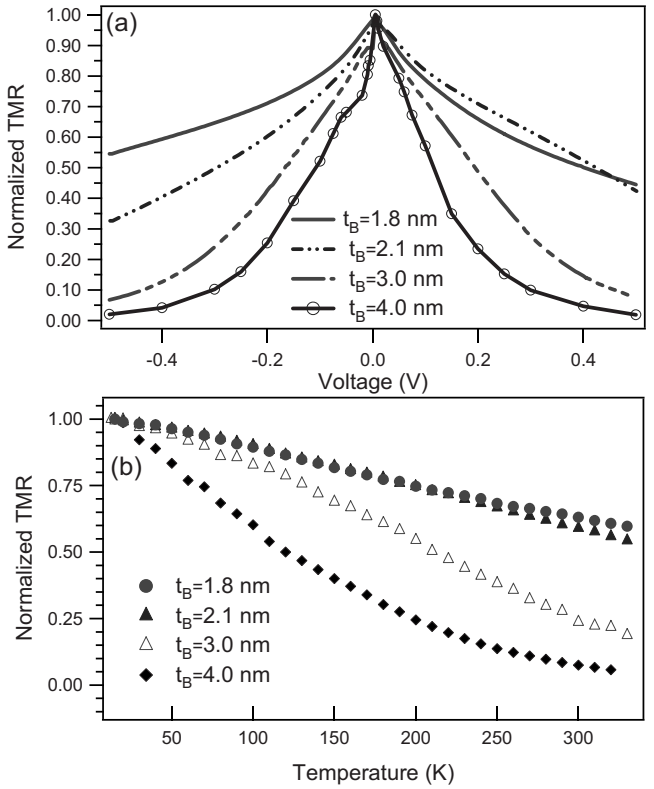

FIG. 2. (a) Typical normalized bias voltage dependence of the TMR for t_B=1.8–4.0 nm measured at 15 K and (b) typical normalized TMR temperature dependence measured with 5 mV bias voltage.

B. Microstructural investigation

To understand the origin for the different bias voltage and temperature dependences for different MgO thickness, microstructural investigations have been performed for t_B=2.1 and 4.0 nm. The transmission electron micrographs of Figs. 3(a) and 3(c) show a good morphology of the MTJ structures with quite smooth interfaces in the overviews. The enlarged HRTEM images in Figs. 3(b) and 3(d) indicate partial crystallization of Co-Fe-B during the postannealing at 350 °C.[24] The MgO tunnel barrier grown on the Co-Fe-B layer showed a good crystalline structure. Moire fringes are observed that point to growth in 5–20 nm sized epitaxial columns with small tilting angles out of plane of the MgO (001)-oriented crystallites.[25] The crystal lattice of the MgO can be clearly identified from the lower interface up to the upper interface for both samples. Therefore, the tunnel barrier and the electrode-barrier interfaces of both junctions seem to be of almost the same quality, which is in accordance with the similar low-temperature/low bias voltage TMR amplitudes of both sample and with the linear barrier thickness dependence of the dielectric breakdown voltage.

TABLE II. Average breakdown voltage U_{BD} (including the statistical error, five MTJs for each barrier thickness) measured at RT in the parallel magnetization state of 225 μm^2 large MTJs for positive bias voltage and a ramp speed of 15 mV/s.

t_B (nm)	U_{BD} (mV)
1.8	1696 ± 13
2.1	1990 ± 15
3.0	2685 ± 20
4.0	3434 ± 22
5.0	4124 ± 38

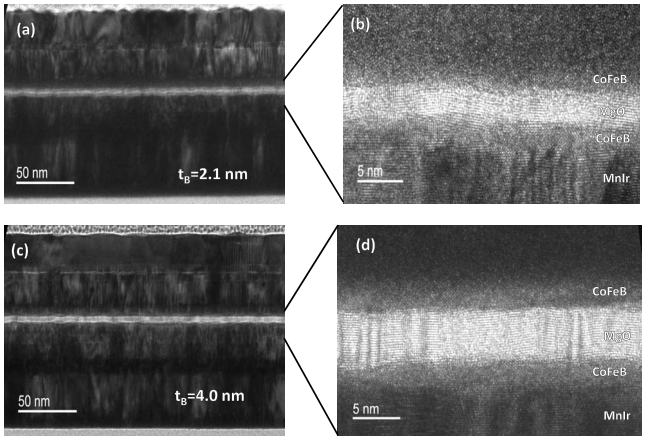

FIG. 3. Transmission electron micrographs of magnetic tunnel junctions. [(a) and (c)] Low magnification image for t_B=2.1 and 4.0 nm. [(b) and (d)] High resolution images for t_B=2.1 and 4.0 nm.

C. Comparison of the experimental data with theoretical models

The bias voltage and temperature dependence of the TMR and the RA products shall now be compared to theoretical models. Drewello *et al.*[26] extended the magnon-assisted tunneling model developed by Zhang *et al.*[27] by thermal smearing and applied it successfully to MgO-based MTJs although coherent tunneling is not explicitly taken into account in this model. The motivation for the extension was the very general experimental result, that the temperature dependence of the resistance in the parallel state in MgO-based junction was so small, that the thermal smearing cannot be assumed to be a second-order process any more. This model is the starting point for our data analysis here. The total conductance for a given temperature T and bias voltage V is described as a sum of the contribution from direct elastic tunneling and from magnon-assisted tunneling,

$$G^{\gamma}(V,T) = G^{\gamma}_{\mathrm{dir}}(V,T) + G^{\gamma}_{\mathrm{mag}}(V,T), \tag{1}$$

where $\gamma=(AP,P)$ describes the magnetic state of the MTJ, $G^{\gamma}_{\mathrm{dir}}(V,T)$ is the direct elastic tunneling conductance and $G^{\gamma}_{\mathrm{mag}}(V,T)$ is the magnon-assisted inelastic conductance. The TMR amplitude is defined as TMR $(V,T)=[G^{P}(V,T) - G^{AP}(V,T)]/G^{AP}(V,T)$. Taking thermal smearing into account the temperature dependence of the total conductance in the limit of zero bias is then given as

$$G^{\gamma}(0,T) = G^{\gamma}(0,0)\frac{CT}{\sin CT}\left[1 + Q\beta^{\gamma}\ln\left(\frac{k_B T}{E_c}\right)\right]. \quad (2)$$

C characterizes the strength of the thermal smearing and is related to the effective barrier thickness d (in Å) and the effective barrier height ϕ (in eV) by $C = 1.387 \times 10^{-4} d/\sqrt{\phi}$. E_c is the low-energy magnon cut-off energy. The parameter β^{γ} is defined as $\beta^{P} = 2Sk_B T\xi/E_m$ and $\beta^{AP} = 2Sk_B T/(\xi E_m)$ for the parallel and the antiparallel magnetic configuration, respectively, with S being the spin parameter and E_m being related to the Curie temperature T_C $[E_m = 3k_B T_C/(S+1)]$ of the ferromagnetic electrode. ξ is the ratio of conductance in both states $\xi = G^{AP}(0,0)/G^{P}(0,0) = R_P(0,0)/R_{AP}(0,0)$. The parameter Q describes the probability that magnons are involved in the tunneling process, it directly depends on the ratio of the squares of the transfer matrix elements for direct (T^d) and magnon-assisted transfer (T^J): $Q = [(|T^d|^2/|T^J|^2) + 2S^2]^{-1}$. The bias voltage dependence of the TMR in the limit of zero temperature is given accordingly as

$$\mathrm{TMR}(V,0) = \mathrm{TMR}(0,0) - Q\frac{SeV}{E_m}\frac{R_{AP}(0,0)}{R_P(0,0)}\left(\frac{1}{\xi} - \xi\right). \quad (3)$$

As mentioned above the temperature and bias voltage dependence becomes much stronger with increasing barrier thickness. More precisely it was not possible to fit the data for $t_B = 2.1$, 3.0, and 4.0 nm self-consistently by Eqs. (2) and (3) only. Therefore, we propose to take an additional unpolarized conductance $G_{UP}(V,T)$ (hopping via localized states) into account, which will lead to very reasonable results. A similar ansatz has been proposed by Shang *et al.*[18] for Al-O-based MTJs. For this, Eq. (1) is amended by an additional term,

$$G^{\gamma}(V,T) = G^{\gamma}_{\mathrm{dir}}(V,T) + G^{\gamma}_{\mathrm{mag}}(V,T) + G_{UP}(V,T). \quad (4)$$

In contrast to the TMR it is obvious that the difference $\Delta G(V,T)$ between the total conductance in the parallel and in the antiparallel state is not changed by this additional unpolarized term. In the limit of zero bias it is given by

$$\Delta G(T) = \frac{CT}{\sin CT}\left\{[G^{P}(0,0) - G^{AP}(0,0)] + \frac{2QSk_B}{E_m}T\left[\xi G^{P}(0,0) - \frac{G^{AP}(0,0)}{\xi}\right]\ln\left(\frac{k_B T}{E_c}\right)\right\}. \quad (5)$$

The self-consistent fitting procedure of our data will now be described. Equation (5) was used to fit $\Delta G(0,T)$ for all four samples *simultaneously* under the constraint that the measured bias voltage dependence of the TMR (average of data for positive and negative bias voltage) for $t_B = 1.8$ nm is reproduced best by Eq. (3) (for this barrier thickness it is known that the magnon-assisted tunneling model can nicely explain the temperature and the bias voltage dependence of the TMR,[26] see also Fig. 4(a). Because of the very similar MgO-barrier interface quality in all junctions (see Sec. III B) the low-energy cut-off energy E_c is expected to be identical for all samples. Furthermore, C is expected to show the mentioned linear dependence on the barrier thickness d and can therefore be rewritten as $C = C' \times d$ with C' being identical

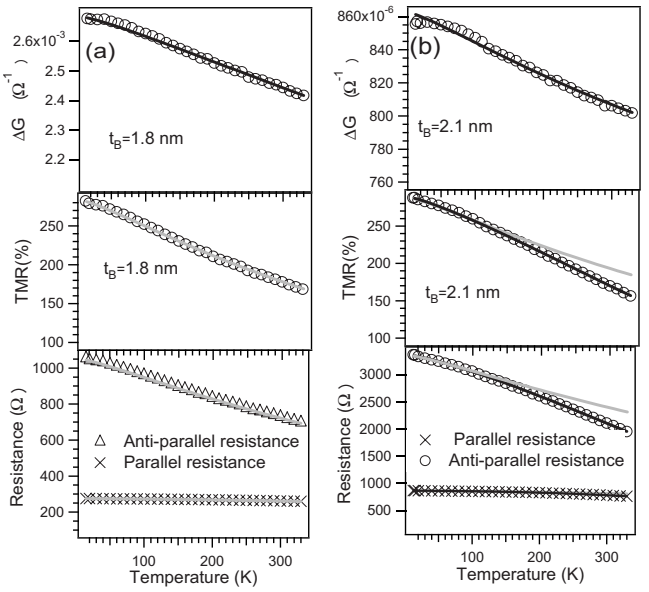

FIG. 4. Typical temperature dependence of ΔG, the TMR, and the resistance for (a) $t_B = 1.8$ nm and (b) 2.1 nm. The junction area is 400 μm^2. The black solid lines are the fits of ΔG according to Eq. (5) and of $R_{P,AP}$ according to Eq. (4). The gray solid lines are the resulting simulations according to Eq. (2), e.g., if only direct and magnon-assisted tunneling would be taken into account.

for all samples. Furthermore, we use individual values of QS/E_m for all samples to account for a possible thickness dependence of this parameter describing the magnon-assisted processes. The results of the self-consistent fits are summarized in Table III.

The fits of Eq. (5) to the experimental $\Delta G(0,T)$ data for $t_B = 1.8$–4.0 nm are shown in the top panels of Figs. 4 and 5. Please note that in contrast to the work by Lu. *et al.*[14] all of our samples show an decreasing $\Delta G(V,T)$ with increasing temperature, we will come back to this below. Finally, please note that the extracted C' value corresponds to a mean barrier height of 4.1 eV which is close to the half of the MgO

TABLE III. Parameters for fitting $\Delta G(0,T)$ by Eq. (5) under the constraint that the bias voltage dependence of the TMR, described by Eq. (3), is reproduced best for $t_B = 1.8$ nm. Technically this was achieved by fixing C' to different values, fitting $\Delta G(0,T)$ for all four samples *simultaneously* and finally checking if the corresponding QS/E_m value for $t_B = 1.8$ nm can reproduce the measured bias voltage dependence of the TMR at low temperature. The best fit of the bias voltage dependence for $t_B = 1.8$ nm and $\Delta G(0,T)$ for all samples was achieved for $C' = 6.85 \times 10^5$ $\mathrm{K}^{-1}\,\mathrm{m}^{-1}$. The corresponding value for the low-energy cut-off energy was $E_c = 0.16 \pm 0.15$ meV.

t_B (nm)	QS/E_m (eV^{-1})
1.8	0.035 ± 0.006
2.1	0.029 ± 0.005
3.0	0.034 ± 0.006
4.0	0.050 ± 0.009

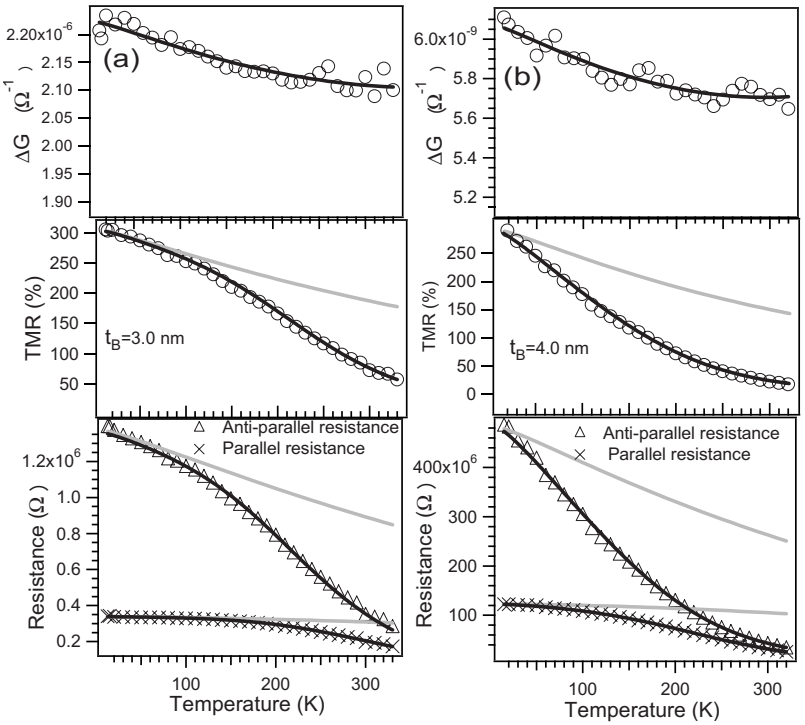

FIG. 5. Typical temperature dependence of ΔG, the TMR, and the resistance for (a) $t_B = 3.0$ nm and (b) 4.0 nm. The junction area is 225 μm^2. The black solid lines are the fits of ΔG according to Eq. (5) and of $R_{P,AP}$ according to Eq. (4). The gray solid lines are the resulting simulations according to Eq. (2), e.g., if only direct and magnon-assisted tunneling would be taken into account.

band gap of 7.8 eV.[28] This gives additional support for the self-consistency of our model.

For $t_B = 1.8$ nm the fitting parameters given in Table III can be inserted in Eq. (2) to reproduce the total conductance $G^{P,AP}(0,T)$ in the parallel and the antiparallel state very well [see black lines in Fig. 4(a)]. This shows that direct spin-polarized and magnon-assisted tunneling dominates the transport for a barrier thickness of 1.8 nm. For $t_B \geq 2.1$ nm the experimental data for $G^{P,AP}(0,T)$ cannot be reproduced in this way (see gray lines Figs. 4 and 5), an additional temperature-dependent current contribution needs to be taken into account now. Because the magnon-assisted tunneling model can self-consistently reproduce ΔG for all samples, this additional current contribution should be unpolarized. It can be calculated by subtracting $G^{P,AP}(0,T)$ according to Eq. (5) from the experimental data. As expected, these differences are nearly identical for parallel and antiparallel alignment (see Fig. 6). In other words this is the justification for the extra term $G_{UP}(V,T)$ in Eq. (4) and the resulting fits can very well reproduce the observed temperature dependence of the TMR and the area resistance products (see black lines in Figs. 4 and 5). The relative contribution of inelastic unpolarized hopping becomes much more important with increasing barrier thickness, as obvious from Fig. 6(d) showing the typical temperature dependence of $G_{UP}(0,T)$ for $t_B = 2.1$, 3.0, and 4.0 nm normalized by $G^P(15\ \mathrm{K})$. This is therefore the reason for the strong decrease in the TMR in these MTJs. In summary, we have shown that the experimental data can be very well explained on the base of direct and magnon-assisted tunneling with an extension by unpolarized hopping conductance. Now we come back to the recent work by Lu *et al.*[14] They have suggested a spin-polarized extension of the inelastic hopping conductance to explain the temperature dependence of the TMR in Co-Fe-B/MgO/Co-Fe-B MTJs. Their main motivation for the assumption of spin-polarized hopping conductance was the experimental observation that $\Delta G(T)$ *increased* with *increasing* temperature for MTJs with 4-nm-thick MgO barrier. We have also applied this model to our data. Details of the procedure can be found in the Appendix. The main results are, that although the temperature-dependent TMR data could be reproduced for all samples quite well, the fit quality for $\Delta G(0,T)$ was worse compared to the extended magnon-assisted tunneling model discussed above. Especially, for $t_B = 4.0$ nm the fit showed a significant deviation from the experimental data for $T > 240$ K and, furthermore, the extracted spin-wave parameters α were different for all samples. The latter would be in contradiction to our microstructural investigations which showed the same quality of the electrode barrier interface for the different samples and, therefore, one would expect the same magnetic interface properties for the different samples.

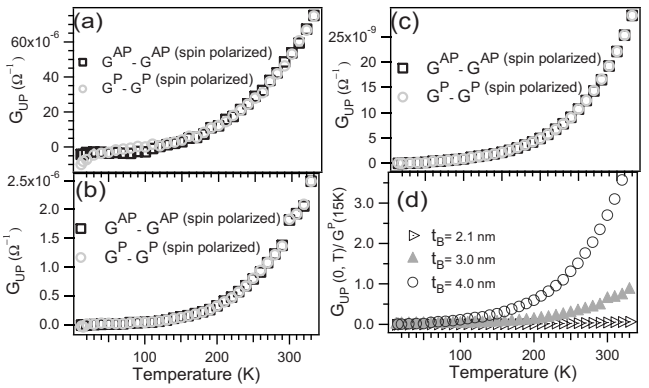

FIG. 6. Typical temperature dependence of $G_{UP}(0,T)$ for (a) $t_B = 2.1$ nm, (b) 3.0 nm, and (c) 4.0 nm. The gray circles (black squares) correspond to the calculation starting with conductance in the parallel (antiparallel) state. In (d) the data resulting from $G^P(0,T)$ are shown after normalization by $G^P(15\ \mathrm{K})$.

Therefore our data cannot be described conclusively by the model by Lu *et al.*[14] Accordingly, the existence of such a polarized conductance channel is not supported by our experiments. On the other hand our model cannot explain the data by Lu *et al.*[14] because in general magnon-assisted tunneling reduces ΔG with increasing temperature. The difference between the samples is not clear at the moment. Especially, differences in the interface quality may be present because the maximal TMR amplitudes at low temperature are different in the two studies. To decide, whether spin-polarized inelastic hopping is of general importance for MgO-based MTJs or not, further comparative studies by other groups are required.

IV. CONCLUSION

We have investigated structural and transport properties of Co-Fe-B/MgO/Co-Fe-B junctions with a barrier thickness of up to 5 nm. HRTEM investigation on junction with barrier thickness t_B=2.1 and 4.0 nm showed a good crystalline quality of the MgO barrier and the electrode-barrier interface for both junction in accordance with the similar low-temperature TMR amplitudes, with the linear dependence of the dielectric breakdown voltage on the barrier thickness and the expected exponential increase in the resistance area product on the barrier thickness. We have demonstrated that direct spin-polarized and magnon-assisted tunneling can explain the bias voltage and temperature-dependent transport properties for a barrier thickness of 1.8 nm, for increasing barrier thickness this model has been successfully extended by an unpolarized current contribution. This additional unpolarized conductance can describe very well the very strong temperature dependence of the TMR for MTJs with 4-nm-thick MgO barrier, and we have not found any hints to spin-polarized inelastic tunneling as observed by Lu *et al.*[14]

ACKNOWLEDGMENTS

The authors gratefully acknowledge financial support by the Deutsche Forschungsgemeinschaft (DFG) and the Bundesministerium für Bildung und Forschung (BMBF). Ayaz Arif Khan acknowledges financial support by the University of Azad Jammu & Kashmir Muzaffarabad (Pakistan). Some of the authors (G.E., M.M., H.S., and M.S.) gratefully acknowledge financial support by the Sonderfoschungsbereich SFB-602.

APPENDIX

In the following we describe the application of the model by Lu *et al.*[14] to our data. This model is based on the spin conserving hopping transport through chains of N-LSs. The first step was to fit the conductance in the antiparallel state by a function of the form

$$G_{AP}(0,T) = \sigma_0 + \sum_{N\geq 2}^{N_{max}} \sigma_N T^{N-2/(N+1)}. \quad \text{(A1)}$$

The parameters σ_N describing the contribution of hopping via N localized states to $G_{AP}(0,T)$ were used as free parameters. For t_B=1.8 and 2.1 nm the data could be fitted by taking chains up to N=2 and N=3, respectively. For t_B =3.0 nm and 4.0 nm higher-order hopping chains were required: for this we have adopted the fitting procedure as Xu *et al.*,[17] i.e., first we restricted the fit to a temperature range that could be fitted best by taking chains up to N=2 only into account. Then the temperature range has been increased so far that it can be best fitted by a function with one additional term and so on. By doing this the data for t_B=3.0 and 4.0 nm in the entire temperature range up to 330 K were fitted with a function containing terms up to N=6 and N=7, respectively. Exemplary results for t_B=1.8 and 4.0 nm are shown in Figs. 7(c) and 7(d). The according relative contribution W_N of different N-LS chains to the antiparallel conductance are shown in Figs. 7(a) and 7(b). Please note that resonant tunneling (N=1) is expected to be T independent and can therefore not be distinguished from direct tunneling (N=0). In this sense the parameter σ_0 must be interpreted as an average value for direct and resonant tunneling.

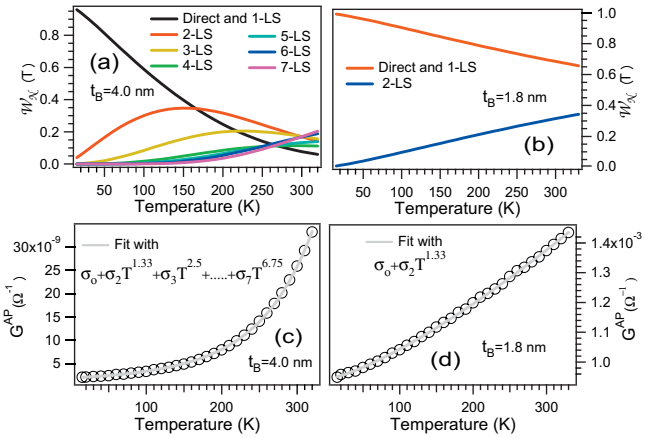

FIG. 7. (Color) Temperature dependence of the tunnel conductance in antiparallel state for (c) t_B=4.0 nm and (d) 1.8 nm and relative contribution $W(N)$ of the different N-LS chains to the antiparallel conductance for (a) t_B=4.0 nm and (b) 1.8 nm.

The expression for $\Delta G(0,T)$ due to the activation of spin conserving inelastic hopping through chains of N localized state at zero bias is given by

TABLE IV. Parameters for fitting $\Delta G(0,T)$ of all samples simultaneously by Eqs. (A2) and (A3). The best simultaneous fits were achieved for $C'=4.0\times10^5$ K^{-1} m^{-1}.

t_B (nm)	P_0	α (K$^{-3/2}$)
1.8	0.7658 ± 0.0004	$5.71\times10^{-6}\pm1.9\times10^{-7}$
2.1	0.7681 ± 0.0004	$4.54\times10^{-6}\pm1.8\times10^{-7}$
3.0	0.7799 ± 0.0004	$6.85\times10^{-6}\pm1.7\times10^{-7}$
4.0	0.7796 ± 0.0004	$1.86\times10^{-5}\pm2.0\times10^{-7}$

$$\Delta G(0,T) = \sigma_0 \frac{CT}{\sin CT} \mathrm{TMR}_0 + \sum_{N\geq 1}^{N_{max}} \sigma_N T^{N-2/(N+1)} \mathrm{TMR}(N,T) \tag{A2}$$

and the $\mathrm{TMR}(N,T)$ assigned to a different variety of chains is given as

$$\mathrm{TMR}(N,T) = \frac{(1+P)^{2\beta_N} + (1-P)^{2\beta_N}}{2(1-P^2)^{\beta_N}} - 1 \tag{A3}$$

with $\beta_N = 1/N+1$ and a T-dependent effective spin polarization $P = P_0(1-\alpha T^{3/2})$, α is the spin-wave parameter related to the interfacial Curie temperature and P_0 is the effective spin polarization at $T=0$ K. The total temperature dependent $\mathrm{TMR}(T)$ is then given as the sum of $\mathrm{TMR}(N,T)$ weighted by their fractional contribution W_N,

$$\mathrm{TMR}(T) = \sum_N W_N(T) \times \mathrm{TMR}(N,T). \tag{A4}$$

Then we fitted the data of all four samples simultaneously by using Eqs. (A2) and (A3), whereas the spin-wave parameters α and the polarizations P_0 were considered as free parameters, and the thermal smearing was taken into account by $C = C' \times d$ with keeping C' identical for all samples. The resulting parameters for $t_B = 1.8-4.0$ nm are given in Table IV, Fig. 8 shows exemplary results for sample A and D. Although the fitting parameters in Table IV can reproduce the temperature-dependent TMR data for all four samples quite well, the fit quality for $\Delta G(0,T)$ was not in all cases as satisfying as by fitting the data by the extended magnon-assisted tunneling model (see Sec. III C). Particularly, for $t_B = 4.0$ nm the fit showed a rising trend of $\Delta G(0,T)$ for $T > 240$ K. Second, the spin-wave parameters α being related to the temperature dependence of the interfacial magnetization and polarization seemed to be different for all samples. But this would be in contradiction to our microstructural investigations which showed the same quality of the electrode barrier interface for junctions with thin and thick barriers.

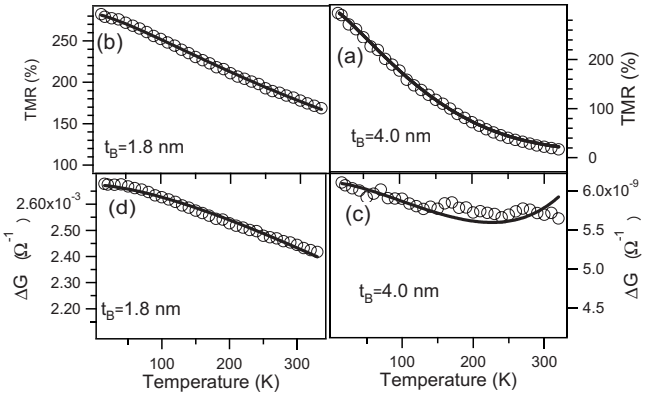

FIG. 8. Typical temperature dependence of $\Delta G(0,T)$ for (c) $t_B = 4.0$ nm and (d) 1.8 nm, the black lines represent fits using Eqs. (A2) and (A3). The black solid lines represent the computed values of $\mathrm{TMR}(T)$ for (a) $t_B = 4.0$ nm and (b) 1.8 nm by inserting the parameters listed in Table IV into Eq. (A4).

*jschmalh@physik.uni-bielefeld.de

[1] S. A. Wolf, D. D. Awschalom, R. A. Buhrman, J. M. Daughton, S. von Molnar, M. L. Roukes, A. Y. Chtchelkanova, and D. M. Treger, Science **294**, 1488 (2001).
[2] M. Julliere, Phys. Lett. A **54**, 225 (1975).
[3] S. S. P. Parkin, C. Kaiser, A. Panchula, P. M. Rice, B. Hughes, M. Samant, and S.-H. Yang, Nature Mater. **3**, 862 (2004).
[4] S. Yuasa, T. Nagahama, A. Fukushima, Y. Suzuki, and K. Ando, Nature Mater. **3**, 868 (2004).
[5] D. D. Djayaprawira, K. Tsunekawa, M. Nagai, H. Maehara, S. Yamagata, N. Watanabe, S. Yuasa, Y. Suzuki, and K. Ando, Appl. Phys. Lett. **86**, 092502 (2005).
[6] Y. M. Lee, J. Hayakawa, S. Ikeda, and H. Ohno, Appl. Phys. Lett. **90**, 212507 (2007).
[7] S. Ikeda, J. Hayakawa, Y. Ashizawa, Y. M. Lee, K. Miura, H. Hasagawa, M. Tsunoda, F. Matsukura, and H. Ohno, Appl. Phys. Lett. **93**, 082508 (2008).
[8] W. H. Butler, X.-G. Zhang, T. C. Schulthess, and J. M. MacLaren, Phys. Rev. B **63**, 054416 (2001).
[9] J. Mathon and A. Umerski, Phys. Rev. B **63**, 220403 (2001).
[10] S. Yuasa, Y. Suzuki, T. Katayama, and K. Ando, Appl. Phys. Lett. **87**, 242503 (2005).
[11] Y. S. Choi, K. Tsunekawa, Y. Nagamine, and D. Djayaprawira, J. Appl. Phys. **101**, 013907 (2007).
[12] J. Y. Bae, W. C. Lim, H. J. Kim, T. D. Lee, and T. W. Kimm, J. Appl. Phys. **99**, 08T316 (2006).
[13] J. Schmalhorst, A. Thomas, G. Reiss, X. Kou, and E. Arenholz, J. Appl. Phys. **102**, 053907 (2007).
[14] Y. Lu, M. Tran, H. Jaffres, P. Seneor, C. Deranlot, F. Petroff, J. M. George, B. Lepine, S. Ababou, and G. Jezequel, Phys. Rev. Lett. **102**, 176801 (2009).
[15] J. C. Read, P. G. Mather, and R. A. Buhrman, Appl. Phys. Lett. **90**, 132503 (2007).
[16] G. X. Miao, Y. J. Park, J. S. Moodera, M. Seibt, G. Eilers, and M. Münzenberg, Phys. Rev. Lett. **100**, 246803 (2008).
[17] Y. Xu, D. Ephron, and M. R. Beasley, Phys. Rev. B **52**, 2843 (1995).
[18] C. H. Shang, J. Nowak, R. Jansen, and J. S. Moodera, Phys. Rev. B **58**, R2917 (1998).
[19] J. Zhang and R. M. White, J. Appl. Phys. **83**, 6512 (1998).
[20] A. A. Khan, J. Schmalhorst, A. Thomas, O. Schebaum, and G. Reiss, J. Appl. Phys. **103**, 123705 (2008).
[21] A. A. Khan, J. Schmalhorst, A. Thomas, V. Drewello, and G. Reiss, J. Appl. Phys. **105**, 083723 (2009).
[22] A. Thomas, V. Drewello, M. Schäfers, A. Weddemann, G. Reiss, G. Eilers, M. Münzenberg, K. Thiel, and M. Seibt, Appl. Phys. Lett. **93**, 152508 (2008).
[23] J. W. McPherson and H. C. Mogul, J. Appl. Phys. **84**, 1513 (1998).
[24] G. Eilers, H. Ulrichs, M. Münzenberg, A. Thomas, K. Thiel, and

M. Seibt, J. Appl. Phys. **105**, 073701 (2009).
[25] G. X. Miao, J. Y. Chang, M. J. van Veenhuizen, K. Thiel, M. Seibt, G. Eilers, M. Münzenberg, and J. S. Moodera, Appl. Phys. Lett. **93**, 142511 (2008).
[26] V. Drewello, J. Schmalhorst, A. Thomas, and G. Reiss, Phys. Rev. B **77**, 014440 (2008).
[27] S. Zhang, P. M. Levy, A. C. Marley, and S. S. P. Parkin, Phys. Rev. Lett. **79**, 3744 (1997).
[28] R. C. Whited, C. J. Flaten, and W. C. Walker, Solid State Commun. **13**, 1903 (1973).